

# Electromagnetic Pion form factor in a deformed background

M. A. Martín Contreras<sup>a,\*</sup>, E. Folco Capossoli<sup>b</sup>, D. Li<sup>c</sup>, A. Vega<sup>a</sup>, and H. Boschi-Filho<sup>d</sup>

<sup>a</sup>*Instituto de Física y Astronomía, Universidad de Valparaíso,  
A. Gran Bretaña 1111, Valparaíso, Chile.*

*\*e-mail: miguelangel.martin@uv.cl*

<sup>b</sup>*Departamento de Física / Mestrado Profissional em Práticas de Educação Básica (MPPEB),  
Colégio Pedro II, 20.921-903 - Rio de Janeiro-RJ - Brazil.*

<sup>c</sup>*Department of Physics and Siyuan Laboratory,  
Jinan University, Guangzhou 510632, China.*

<sup>d</sup>*Instituto de Física, Universidade Federal do Rio de Janeiro,  
21.941-972 - Rio de Janeiro-RJ - Brazil.*

Received 11 January 2022; accepted 21 March 2022

This work discusses the electromagnetic (EM) pion form factor ( $\pi FF$ ) in a deformed AdS geometry. We consider the conformal dimension of the hadron bulk field defined by the scaling dimension of the  $q\bar{q}$  operator instead of the twist. We also compute the pion EM radius and compare it with the experimental data, finding a relative error of 2%.

*Keywords:* Deformed string/gauge correspondence; AdS/QCD; pion form factor.

DOI: <https://doi.org/10.31349/SuplRevMexFis.3.0308079>

## 1. Introduction

Electromagnetic pion form factor ( $\pi FF$ ) is one of the most valuable QCD quantities related to the transition from the non-perturbative to the perturbative regime. From theoretical studies such as [1], it is expected the emergence of a *Sudakov suppression* in the  $\pi FF$  for intermediate  $q^2$  regions. In this work, we want to explore this phenomenology from holographic grounds.

In general, the primary motivation behind the AdS/QCD idea is how we place confinement. In pure AdS space, bulk fields are conformal. Free bulk fields have normalizable modes with continuous eigenspectra. Thus, they are not a good choice to describe hadrons. To circumvent this issue, we can add geometrical deformations to the background. In this top/down scenario, the equivalence with low energy QCD appears when we consider equally the conformal boundary theory and QCD coupling constants at some fixed point. However, this prescription is restrictive. For instance, these models do not have fundamental degrees of freedom *ab initio*. They should be added by geometrical deformations, such as another stack of D-branes, whose Chan-Paton charge corresponds with the number of flavors of the theory [2].

Another possibility to address the emergence of bounded (hadronic) states in holography is directly transforming the continuous bulk eigenspectrum into a discrete one. This idea is achieved by slightly breaking the conformal invariance in the bulk. We can do this in two forms: by placing a dilaton (the so-called softwall [3] model) or deforming the geometry (the hardwall [4–7] and the deformed background models [8, 9]). Consequently, we will obtain a dual radial Regge

trajectory, which can be linear if the dilaton or deformation are chosen to be quadratic in the holographic coordinate. We will follow the latter path.

This work is organized as follows: in Sec. 2, we describe the deformed background model for pions and photon. In Sec. 3, we summarize the holographic  $\pi FF$  calculation in terms of bulk interacting fields. Finally, in Sec. 4 we present our conclusions.

## 2. Deformed Background Model

Let us consider a general five-dimensional AdS background defined by

$$dS^2 = \frac{R^2}{z^2} e^{2h(z)} [dz^2 + \eta_{\mu\nu} dx^\mu dx^\nu], \quad (1)$$

where  $R$  defines the AdS curvature radius, and the Greek indices label four-dimensional spacetime indices. The geometrical deformation  $h(z)$  sets confinement.

Hadrons are defined using the bulk fields defined by the action

$$I_{\text{Hadron}} = \int d^5x e^{-\Phi(z)} \mathcal{L}_{\text{Hadron}}, \quad (2)$$

where  $\Phi(z)$  is a dilaton (which can be statically or dynamically generated) which also induces confinement. The lagrangian  $\mathcal{L}_{\text{Hadron}}$  carries all the relevant information of how bulk fields will mimic hadrons at the boundary.

From the metric (1) and the action (2), we can write bulk equations of motion. These equations are transformed into a Schrodinger-like eigenvalue problem  $-\psi'' + V(z)\psi = M_n^2 \psi$ , with the  $V(z)$  defined as holographic potential, and  $\psi(z)$  the normalizable part of the bulk field dual to hadrons.

In general, the holographic potential for integer spin hadrons has the form

$$V(z) = \frac{1}{4} B'(z)^2 - \frac{1}{2} B''(z) + \frac{M_5^2 R^2}{z^2} e^{2h(z)}, \quad (3)$$

where we have introduced  $B(z) = \Phi(z) + \beta [\log(R/z) + h(z)]$ , and  $M_5^2 R^2$  defines the bulk field mass, which characterizes the hadronic identity in terms of its conformal dimension. The information initially captured in the bulk action (2) is now translated into the  $B(z)$  function. The parameter  $\beta$  counts the hadronic spin in  $3 + 1$  dimensions. For scalar hadrons we have  $\beta = -3$ , and for vectors we have  $\beta = -1$ . The eigenspectrum  $M_n^2$  obtained from this holographic potential defines the so-called *holographic Regge trajectories*.

The geometric background model introduced in Refs. [9, 10] emerges when we fix  $\Phi(z) = 0$  and  $h(z) = (1/2) k z^2$ . Notice that the parameter  $k$  is flavor dependent, *i.e.*, each particle in the model has its own geometric background.

### 2.1. Pions in the deformed background model

Pions are defined by a bulk massive scalar field  $X$  obeying the following action

$$I_\pi = \int d^5x \sqrt{-g_\pi} [g_\pi^{mn} \partial_m X \partial_n X + M_5^2 X^2], \quad (4)$$

where the bulk mass  $M_5^2$  is defined in terms of the scalar conformal dimension  $\Delta$  as follows

$$M_5^2 R^2 = \Delta(\Delta - 4). \quad (5)$$

For hadrons,  $\Delta$  is identified with the dimension of the operator creating them at the boundary. In the case of mesons, they are created by the operator  $q\bar{q}$ , whose dimension is three. Therefore, in this particular case, the bulk mass is  $M_5^2 R^2 = -3$ .

From the action (4) we obtain the following equation of motion for the  $X$  field:

$$\partial_z \left[ e^{-B_\pi(z)} \partial_z X \right] + M_n^2 e^{-B_\pi(z)} X + \frac{3R^2}{z^2} e^{\frac{1}{2} k_\pi z^2} X = 0, \quad (6)$$

where we have imposed the on-shell condition  $-q^2 = M_n^2$  for the pion, and also we have defined  $B_\pi(z) = -3 \log(R/z) - (3/2) k_\pi z^2$ .

Following the standard bottom-up AdS/QCD prescription [3, 11–13], after performing the transformation  $X(z) = e^{\frac{1}{2} B_\pi(z)} \psi_{\pi,n}(z)$  we can write the following holographic potential (3) for the pion normalizable bulk modes  $\psi_{\pi,n}(z)$  as

$$V_\pi(z) = \frac{15}{4z^2} - \frac{3}{z^2} e^{-k_\pi z^2} + \frac{k_\pi^2 z^2}{4} + k_\pi. \quad (7)$$

The ground state of this potential is identified with the pion. Thus, using the pion mass, we can fit the value of deformation slope as  $k_\pi = -0.0425^2 \text{ GeV}^2$ .

### 2.2. Virtual photons in the deformed background model

Virtual photons emerge from the non-normalizable part of an abelian massless vector bulk field  $\phi_m(z, q)$ , defined by the action

$$I_\gamma = -\frac{1}{\alpha_\gamma^2} \int d^5x \sqrt{-g_\gamma} \frac{1}{4} F^{mn} F_{mn}, \quad (8)$$

where  $\alpha_\gamma$  is a coupling constant setting units in the action, and  $F_{mn} = 2 \partial_{[m} \phi_{n]}$  is field strength, and  $\phi_\mu$  is a bulk abelian vector field.

At the conformal boundary, the vector field should behave as transverse wave, *i.e.*,  $\phi_\mu(x, z \rightarrow 0) = \eta_\mu e^{-i q \cdot x}$ . This condition imposes that  $\phi_z = 0$ . Thus, the bulk vector field will be written as

$$\phi_\mu(z, q) = \eta_\mu e^{-i q \cdot x} \mathcal{B}(z, q), \quad (9)$$

where  $\mathcal{B}(z, q)$  is the so-called *bulk-to-boundary propagator*. From the vector field action we can write the equations of motion for  $\mathcal{B}(z, q)$  as follows

$$\partial_z \left[ e^{-B_\gamma(z, q)} \partial_z \mathcal{B}(z, q) \right] - q^2 e^{-B_\gamma(z)} \mathcal{B}(z, q) = 0, \quad (10)$$

where  $B_\gamma(z) = -\log(R/z) - (1/2) k_\gamma z^2$ . The equation for the bulk-to-boundary propagator has the following solution

$$\mathcal{B}(z, q) = -\frac{1}{2} k_\gamma z^2 \Gamma \left[ 1 - \frac{q^2}{2k_\gamma} \right] \times \mathcal{U} \left( 1 - \frac{q^2}{2k_\gamma}; 2; -\frac{k_\gamma z^2}{2} \right), \quad (11)$$

where  $\mathcal{U}(a, b, z)$  is the Tricomi function, and  $k_\gamma$  is the energy scale associated with the virtual photon kinematics.

Now that we have described the holographic ingredients, we can move towards the holographic calculation of the pion form factor.

### 3. Holographic $\pi$ FF calculation

In holography, form factors are defined via interaction terms in the bulk action (2). These interaction terms may arise in two possible forms. One is from high-order expansions in the bulk lagrangian, encoded in the group covariant derivatives due to the inner group structure associated with the bulk fields [14]. The other comes from phenomenological interaction terms written *ab initio* inspired by expected hadronic properties, such as sum rules or OPE's [15].

In this scenario, the electromagnetic form factor comes from the minimal coupling between scalar bulk field normalizable Schrodinger modes (dual to the incoming and outgoing pions) and a vector bulk field non-normalizable part  $\mathcal{B}(z, q^2)$  (dual to the virtual photon). Therefore we have [16]

$$F_\pi(q^2) = \int dz \psi_{\pi,1}(z) \mathcal{B}(z, q^2) \psi_{\pi,1}(z), \quad (12)$$

where  $\psi_{\pi,1}(z)$  stands for the pion ground state eigenfunction.

In our particular case, since we have a background for each particle, we have set (*or choose*) the frame where we will calculate the interaction term (12). In this sense, we propose the *pion geometric background* as the most natural scenario, since in this frame, we have defined the pion Schrodinger-like modes.

This explicit form for the  $\pi$ FF was introduced in the context of light-front (LF) holography [15], where  $\Delta$  is not associated with the dimension of the operator creating hadrons. Instead,  $\Delta$  is connected with the *twist*, which carries the particle content information. Thus, in the case of mesons,  $\Delta = \tau = 2$ . With this choice, the  $\pi$ FF has the correct large  $q^2$  behavior, expected from QCD sum rules [29]. In the next paragraphs, we will explore the case with  $\Delta = 3$ , outside the LF holography context.

### 3.1. $k_\gamma$ fixed case

As usual in AdS/QCD, we will take the conformal dimension for the scalar bulk field as  $\Delta = 3$ . In Fig. 1 we summarize our results comparing with experimental and theoretical (holographic and non-holographic) available data. To test the consistency with the sum rules, we will examine the Brodsky-Lepage counting rule calculated in this model:

$$F_\pi(q^2)|_{q^2 \rightarrow \infty} = \frac{1 + \gamma_e(\Delta - 1)\Delta + \dots}{8\Delta^2(\Delta - 1)} \times \left(\frac{1}{q^2}\right)^{\Delta-1} \propto \frac{1}{q^4}. \quad (13)$$

Notice that when we consider the LF case, *i.e.*  $\Delta = 2$  [15], we recover the expected behavior  $1/q^2$  for the  $\pi$ FF. However, in the non-LF case, our geometric deformed background model with  $\Delta = 3$  and using Eq. (12), we observed

that the  $\pi$ FF captures the low  $q^2$  (below 1 GeV<sup>2</sup>) behavior (see Fig. 1), nevertheless it does not satisfy the expected counting rule. The  $\pi$ FF in this situation is highly suppressed for high  $q^2$  values also.

The low  $q^2$  behavior is tested by calculating the pion electromagnetic radius, defined as

$$\langle r_\pi^2 \rangle = -6 \left. \frac{dF_\pi(q^2)}{dq^2} \right|_{q^2=0}. \quad (14)$$

In this situation with  $\Delta = 3$  and  $k_\gamma = -3.8$  GeV<sup>2</sup>, we obtain  $r_\pi = 0.458$  fm, with an error around 30% compared with experimental data [30].

### 3.2. $k_\gamma$ running with $q$ case

A possible form to circumvent this issue with the counting rule appears when we assume the photon slope  $k_\gamma$  to be a function of the transferred momentum  $q$ . The parameter  $k_\gamma$  does not set confinement, and it is related with the kinematic scale of the virtual photon. Thus, we will fix  $k_\gamma(q) = q\kappa_\gamma$ , where  $\kappa_\gamma$  has energy units. If we compute the  $\pi$ FF at large  $q^2$ , following the procedure described in Ref. [15],

$$F_\pi(q^2)|_{q^2 \rightarrow \infty} = \frac{32k_\gamma^2(q)}{[q^2 + 4|k_\gamma(q)|][q^2 + 8|k_\gamma(q)|]} \propto \frac{1}{q^2}, \quad (15)$$

we will fulfill the Brodsky-Lepage rule. The results in this situation are depicted in Fig. 2. Notice that we also have a softened Sudakov suppression, as expected from lattice analysis. The plots also show that this approach captures the low  $q^2$  phenomenology. When we compute the pion electromagnetic radius with  $\kappa_\gamma = -2.8$  GeV, we obtain  $r_\pi = 0.671$ , having 2% of error compared with experimental data [30].

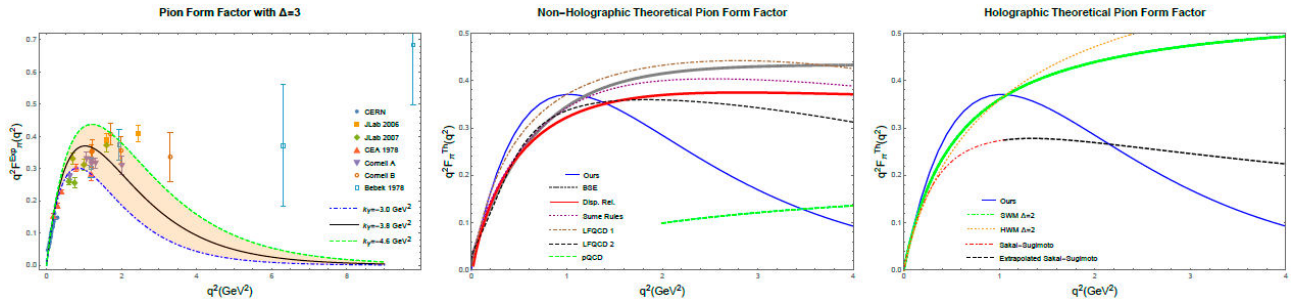


FIGURE 1. The left panel compares our results for the pion form factor with the available experimental data [17–22]. In the next panels, we have a comparison of our results with non-holographic models (center panel) such as BSE [23], perturbative QCD [25], dispersion relations [26], sum rules [27], and LFQCD [1]. In the right panel, we depict a comparison with other holographic models such as hardwall and softwall with  $\Delta = 2$  [15], and Sakai-Sugimoto/extrapolated Sakai-Sugimoto [28]. In our results we have taken  $k_\gamma = -3.8$  GeV<sup>2</sup>.

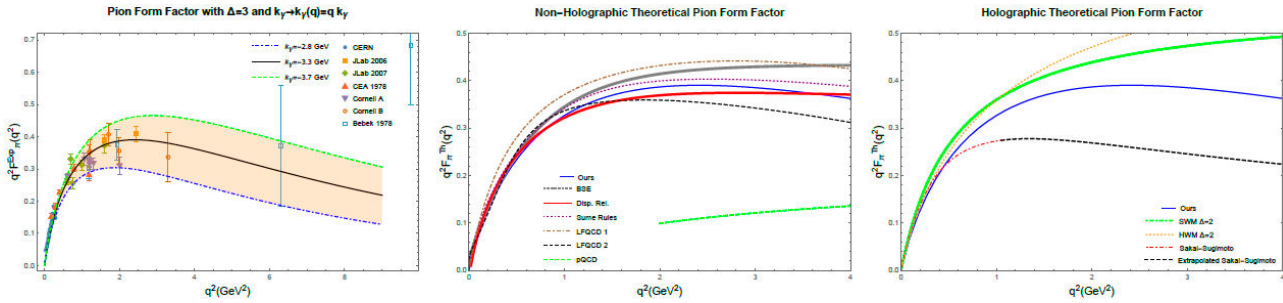


FIGURE 2. The left panel compares our results for the pion form factor with the available experimental data [17–22] using the proposed scaling for  $k_\gamma$ . In the next panels, we depict a comparison of our results with non-holographic models (center panel) such as BSE [23] or Light-Front BSE [24], perturbative QCD [25], dispersion relations [26], sum rules [27], and LFQCD [1]. In the right panel, we show a comparison with other holographic models such as hardwall and softwall with  $\Delta = 2$  [15], and Sakai-Sugimoto/extrapolated Sakai-Sugimoto [28]. In our results, for lower panels we have taken  $k_\gamma = -2.8 \text{ GeV}^2$ .

## 4. Conclusions

In this work, we have calculated the electromagnetic pion form factor holographically by considering non-LF formalism, *i.e.*, we have considered  $\Delta = 3$ . We show the issue with the large  $q^2$  behavior that this prescription has and how to solve it by considering a re-scaling in the photon slope  $k_\gamma$  that sets the corresponding geometric background. Our calculation captures the low  $q^2$  behavior and also exhibits a Sudakov-like suppression in the intermediate  $q^2$  region, as it was suggested by lattice [1]. Our calculation of the pion electromagnetic radius give us a result of 0.671 fm, with a 2% error in comparison with available experimental data.

## Acknowledgments

A. V. and M. A. M. C. would like to thank the financial support given by FONDECYT (Chile) under Grants No. 1180753 and No. 3180592, respectively. D.L. is supported by the National Natural Science Foundation of China (11805084), the PhD Start-up Fund of Natural Science Foundation of Guangdong Province (2018030310457) and Guangdong Pearl River Talents Plan (2017GC010480). H.B.-F. is partially supported by Coordenação de Aperfeiçoamento de Pessoal de Nível Superior (CAPES), and Conselho Nacional de Desenvolvimento Científico e Tecnológico (CNPq) under Grant No. 311079/2019-9.

1. H. M. Choi and C. R. Ji, Conformal symmetry and pion form-factor: Soft and hard contributions, *Phys. Rev. D* **74** (2006) 093010, <https://doi.org/10.1103/PhysRevD.74.093010>.
2. J. Erdmenger, N. Evans, I. Kirsch and Threlfall, Mesons in Gauge/Gravity Duals - A Review, *Eur. Phys. J. A* **35** (2008) 81-133, <https://doi.org/10.1140/epja/i2007-10540-1>.
3. A. Karch, E. Katz, D. T. Son and M. A. Stephanov, Linear confinement and AdS/QCD, *Phys. Rev. D* **74** (2006) 015005, <https://doi.org/10.1103/PhysRevD.74.015005>.
4. H. Boschi-Filho and N. R. F. Braga, QCD / string holographic mapping and glueball mass spectrum, *Eur. Phys. J. C* **32** (2004) 529-533, <https://doi.org/10.1140/epjc/s2003-01526-4>.
5. J. Erlich, E. Katz, D. T. Son and M. A. Stephanov, QCD and a holographic model of hadrons, *Phys. Rev. Lett.* **95** (2005) 261602, <https://doi.org/10.1103/PhysRevLett.95.261602>.
6. N. R. F. Braga, M. A. Martín Contreras and S. Diles, Decay constants in soft wall AdS/QCD revisited, *Phys. Lett. B* **763** (2016) 203-207, <https://doi.org/10.1016/j.physletb.2016.10.046>.
7. M. A. Martín Contreras and A. Vega, Nonlinear Regge trajectories with AdS/QCD, *Phys. Rev. D* **102** (2020) 046007, <https://doi.org/10.1103/PhysRevD.102.046007>.
8. H. Forkel, M. Beyer and T. Frederico, Linear square-mass trajectories of radially and orbitally excited hadrons in holographic QCD, *JHEP* **07** (2007) 077, <https://doi.org/10.1088/1126-6708/2007/07/077>.
9. E. Folco Capossoli, M. A. Martín Contreras, D. Li, A. Vega and H. Boschi-Filho, Hadronic spectra from deformed AdS backgrounds, *Chin. Phys. C* **44** (2020) 064104, <https://doi.org/10.1088/1674-1137/44/6/064104>.
10. E. Folco Capossoli, M. A. Martín Contreras, D. Li, A. Vega and H. Boschi-Filho, Proton structure functions from an AdS/QCD model with a deformed background, *Phys. Rev. D* **102** (2020) 086004, <https://doi.org/10.1103/PhysRevD.102.086004>.
11. T. Gutsche, V. E. Lyubovitskij, I. Schmidt and A. Vega, Dilaton in a soft-wall holographic approach to mesons and baryons, *Phys. Rev. D* **85** (2012) 076003, <https://doi.org/10.1103/PhysRevD.85.076003>.
12. M. Á. Martín Contreras, A. Vega and S. Cortés, Light pseudoscalar and axial spectroscopy using AdS/QCD modified soft wall model, *Chin. J. Phys.* **66** (2020) 715-723, <https://doi.org/10.1016/j.cjph.2020.06.018>.

13. P. Colangelo, F. De Fazio, F. Giannuzzi, F. Jugeau and S. Nicotri, Light scalar mesons in the soft-wall model of AdS/QCD, *Phys. Rev. D* **78** (2008) 055009, <https://doi.org/10.1103/PhysRevD.78.055009>.
14. H. J. Kwee and R. F. Lebed, Pion form-factors in holographic QCD, *JHEP* **01** (2008) 027, <https://doi.org/10.1088/1126-6708/2008/01/027>.
15. S. J. Brodsky and G. F. de Teramond, Light-Front Dynamics and AdS/QCD Correspondence: The Pion Form Factor in the Space- and Time-Like Regions, *Phys. Rev. D* **77** (2008) 056007, <https://doi.org/10.1103/PhysRevD.77.056007>.
16. M. A. Martin Contreras, E. Folco Capossoli, D. Li, A. Vega and H. Boschi-Filho, *Pion form factor from an AdS deformed background*,
17. H. Ackermann, *et al.*, Determination of the Longitudinal and the Transverse Part in  $\pi^+$  Electroproduction, *Nucl. Phys. B* **137** (1978) 294-300, [https://doi.org/10.1016/0550-3213\(78\)90523-0](https://doi.org/10.1016/0550-3213(78)90523-0).
18. C. J. Bebek, *et al.* Electroproduction of single pions at low  $\epsilon$  and a measurement of the pion form-factor up to  $q^2 = 10\text{-GeV}^2$ , *Phys. Rev. D* **17** (1978) 1693, <https://doi.org/10.1103/PhysRevD.17.1693>.
19. P. Brauel, *et al.*, Electroproduction of  $\pi^+n$ ,  $\pi^-p$  and  $K^+\Lambda$ ,  $K^+\Sigma^0$  Final States Above the Resonance Region, *Z. Phys. C* **3** (1979) 101, <https://doi.org/10.1007/BF01443698>.
20. S. R. Amendolia *et al.* [NA7], A Measurement of the Space - Like Pion Electromagnetic Form-Factor, *Nucl. Phys. B* **277** (1986) 168, [https://doi.org/10.1016/0550-3213\(86\)90437-2](https://doi.org/10.1016/0550-3213(86)90437-2).
21. T. Horn *et al.* [Jefferson Lab F(pi)-2], Determination of the Charged Pion Form Factor at  $Q^{*2} = 1.60$  and  $2.45\text{-(GeV/c)}^{*2}$ , *Phys. Rev. Lett.* **97** (2006) 192001, <https://doi.org/10.1103/PhysRevLett.97.192001>.
22. V. Tadevosyan *et al.* [Jefferson Lab F(pi)], Determination of the pion charge form-factor for  $Q^{*2} = 0.60\text{-GeV}^{*2} - 1.60\text{-GeV}^{*2}$ , *Phys. Rev. C* **75** (2007) 055205, <https://doi.org/10.1103/PhysRevC.75.055205>.
23. P. Maris and P. C. Tandy, The  $\pi$ ,  $K^+$ , and  $K^0$  electromagnetic form-factors, *Phys. Rev. C* **62** (2000) 055204, <https://doi.org/10.1103/PhysRevC.62.055204>.
24. C. Shi, K. Bednar, I. C. Cloët and A. Freese, Spatial and Momentum Imaging of the Pion and Kaon, *Phys. Rev. D* **101** (2020) 074014, <https://doi.org/10.1103/PhysRevD.101.074014>.
25. A. P. Bakulev, *et al.*, Pion form-factor in QCD: From nonlocal condensates to NLO analytic perturbation theory, *Phys. Rev. D* **70** (2004) 033014, [erratum: *Phys. Rev. D* **70** (2004) 079906], <https://doi.org/10.1103/PhysRevD.70.033014>.
26. B. V. Geshkenbein, Pion electromagnetic form-factor in the space - like region and P phase  $\delta(1)$  in one-dimension (s) of  $\pi\pi$  scattering from the value of the modulus of form-factor in the time - like region., *Phys. Rev. D* **61** (2000) 033009, <https://doi.org/10.1103/PhysRevD.61.033009>.
27. V. A. Nesterenko and A. V. Radyushkin, Sum Rules and Pion Form-Factor in QCD, *Phys. Lett. B* **115** (1982) 410, [https://doi.org/10.1016/0370-2693\(82\)90528-7](https://doi.org/10.1016/0370-2693(82)90528-7).
28. C. A. B. Bayona, H. Boschi-Filho, M. Ihl and M. A. C. Torres, Pion and Vector Meson Form Factors in the Kuperstein-Sonnenschein holographic model, *JHEP* **08** (2010) 122, [https://doi.org/10.1007/JHEP08\(2010\)122](https://doi.org/10.1007/JHEP08(2010)122).
29. S. J. Brodsky and G. R. Farrar, Scaling Laws at Large Transverse Momentum, *Phys. Rev. Lett.* **31** (1973) 1153-1156, <https://doi.org/10.1103/PhysRevLett.31.1153>.
30. P.A. Zyla *et al.*, (Particle Data Group), *Prog. Theor. Exp. Phys.* **2020** (2020) 083C01.